High-energy and efficient Raman soliton generation tunable from 1.98 to 2.29 μm in an all-silica-fiber thulium laser system

JINZHANG WANG,[1] SHENGHUA LIN,[1] XIAOYAN LIANG,[1] MENGMENG WANG,[1] PEIGUANG YAN,[1] GUOHUA HU,[2] TOM ALBROW-OWEN,[2] SHUANGCHEN RUAN,[1,*] ZHIPEI SUN,[3] TAWFIQUE HASAN[2]

[1]*Shenzhen Key Laboratory of Laser Engineering, College of Optoelectronic Engineering, Shenzhen University, Shenzhen 518060, China*
[2]*Cambridge Graphene Centre, University of Cambridge, Cambridge CB3 0FA, United Kingdom*
[3]*Department of Micro- and Nanosciences, Aalto University, Aalto, FI-00076, Finland*
**Corresponding author: scruan@szu.edu.cn*

Received XX Month XXXX; revised XX Month, XXXX; accepted XX Month XXXX; posted XX Month XXXX (Doc. ID XXXXX); published XX Month XXXX

We demonstrate a compact, all-fiber-integrated laser system that delivers Raman solitons with a duration of ~100 fs and pulse energy of up to 13.3 nJ, continuously wavelength tunable from 1.98 to 2.29 μm via Raman-induced soliton self-frequency shift (SSFS) in a thulium-doped fiber amplifier. We realize a >90% efficiency of Raman conversion, the highest reported value from SSFS-based sources. This enables us to achieve >10 nJ soliton energy from 2.16 to 2.29 μm range, the highest energy demonstrated above 2.22 μm from an SSFS-assisted all-fiber tunable single-soliton-pulse source. Our simple and compact all-fiber tunable laser could serve as an efficient ~2 μm femtosecond source for a wide range of mid-IR applications.

OCIS codes: *(060.2320) Fiber optics amplifiers and oscillators; (320.7090) Ultrafast lasers; (060.4370) Nonlinear optics, fibers; (060.5530) Pulse propagation and temporal solitons.*

http://dx.doi.org/10.1364/OL.99.099999

High energy tunable femtosecond pulses at the 2 μm region are of great interest for many scientific and industrial applications. For example, they can be used for nonlinear frequency conversion towards the mid-infrared "molecular fingerprint" region [1]. Frequency doubling to the 1 μm region can replace the current Yb- or Nd-doped tunable light sources. A broadband tunability at ~2 μm regime is very useful for sensing many atmospheric molecules, such as CO_2 and H_2O [2]. In addition, strong absorption lines of water molecules at this region enable these sources to be useful for surgical applications since the human body contains >60% H_2O. Other applications include material processing, high resolution ultrafast spectroscopy and eye-safe LIDAR [3]. We also note that for many applications outside the laboratory, fiber-based femtosecond sources have clear advantages compared to the bulk solid-state lasers in terms of compactness, inherently high beam quality, and environmental reliability.

Thulium (Tm) doped gain fibers offer a broad gain bandwidth between 1.8-2.1 μm, supporting ultrashort pulse generation as well as wide wavelength tunability [4-6]. Over the past decades, they have been used to demonstrate generation of broadly tunable femtosecond pulses in this spectral region [7, 8]. Up to 200 nm wavelength tuning range has been directly achieved in a Tm fiber oscillator, with pulse energy <1 nJ [9]. However, wavelength tunability for >2.1 μm is restricted by the Tm gain bandwidth. Raman scattering (*e.g.*, stimulated Raman scattering [10, 11] and Raman-induced soliton self-frequency shift (SSFS) [12]) is an effective way to extend the light sources to longer wavelength. Especially, the SSFS in non-silica or silica based fibers could produce high-quality femtosecond Raman solitons over a wide wavelength range beyond 2.1 μm [13-16]. Compared to the non-silica based fibers, silica fibers generally have lower cost, and support much higher energy and average power due to their lower nonlinearity [5]. In addition, direct fusion splicing between silica fibers enables construction of reliable and robust all-fiber systems, compatible to the current well-developed silica fiber systems.

A silica-based Tm fiber amplifier can act as both the Raman shifter and amplifier, capable of generating high energy tunable Raman solitons beyond the upper limit of Tm gain bandwidth [17, 18]. ~100 fs pulses with wavelength tunability from 1.93 to 2.2 μm and pulse energy as high as 5 nJ were directly generated from a single-stage Tm fiber amplifier [19]. The highest soliton energy produced from an SSFS-assisted fiber source was reported in Ref. [20], where a compact Tm-based fiber laser system delivered tunable solitons in the 2-2.2 μm range, with pulse energy of up to 38 nJ at 2.15 μm. However, due to the increasing absorption of host

silica, it is usually challenging to effectively extend the wavelength beyond 2.22 μm via SSFS in Tm fiber amplifier [17-21]. Larger SSFS could usually result in the decrease in soliton energy [22], and be accompanied by the birth of second tunable soliton pulse and spectral distortion of the first soliton [16, 21]. Such new spectral components gradually lead to supercontinuum generation [16].

In this Letter, we demonstrate a compact and simple all-silica-fiber Tm tunable laser system to produce femtosecond solitons in the 1.98-2.29 μm range with 55.42 MHz repetition rate. Over the tuning range, no distinguishable second soliton is observed, and the Raman solitons are nearly Fourier limited, with pulse duration between 95 and 290 fs and energy between 1.45 and 13.3 nJ. In the 2.16-2.29 μm tuning range, the achieved soliton energy is higher than 10 nJ. This is, to our knowledge, the first demonstration of >10 nJ solitons beyond 2.22 μm without the birth of second soliton from an SSFS-assisted all-fiber tunable laser source. This is attributed to the large conversion efficiency of Raman soliton, which is defined as the ratio of the red-shifted soliton energy to the total pulse energy. Our highest conversion efficiency is 91.5%, significantly exceeding the previously reported maximum value of 62.5% [17] from Tm-based SSFS fiber sources.

The experimental setup of the all-fiber Tm based laser system is depicted in Fig. 1. It comprises a seed oscillator and a two-stage all-fiber amplifier. The oscillator consists of a short piece of (~16 cm) highly Tm doped fiber (TDF, Nufern SM-TSF-5/125), a 1550/1940 nm wavelength division multiplexer, an output coupler, a carbon nanotube based saturable absorber (CNT-SA) and a polarization insensitive isolator. Pump light is provided by a commercial Er fiber amplifier that emits at ~1550 nm. The isolator is used to ensure unidirectional light propagation in the cavity. A 20% fraction of intra-cavity light is coupled to the output port. The CNT-SA has the modulation depth of ~10% and a saturation influence of 18 μJ/cm^2 at ~1.9 μm [23]. More details on the fabrication and characterization of CNT-SA can be found in our previous works [24, 25]. All the passive fibers in the oscillator are composed of standard telecom single mode fiber (SMF-28e) which has negative dispersion of ~ −71 ps^2/km at 1.9 μm [26]. The total cavity length is ~3.72 m, which corresponds to a ~55.4 MHz repetition rate.

The seed pulse signal is then sent to the two-stage amplifier. A polarization controller (PC) placed between the oscillator and amplifier can compensate the nonlinear phase shift induced by the amplifier for stabilizing and optimizing the Raman soliton. The first-stage amplifier named preamplifier has the well-known structure of chirped pulse amplification (CPA), where a segment of normal dispersion compensating fiber (DCF) is used before the gain fiber to stretch the pulse. We use a 3.5 m long ultrahigh NA fiber (Nufern, NUHA4) with a small core diameter of 2.2 μm as DCF, exhibiting normal dispersion of 93 ps^2/km at 1.9 μm [27]. The following active fiber is a 0.8 m long double cladding (DC) TDF (Nufern, SM-TDF-10P/130) core-pumped by another commercial Er fiber amplifier. The second-stage amplifier is employed to act as both the amplifier for boosting the output power and Raman shifter for realizing Raman-induced SSFS. It is comprised of a 1.5 m long DC-TDF (Coractive, DCF-TM-12/128P) with a large core diameter of 12 μm, forward clad-pumped by a high power 794 nm multimode laser diode through a silica based pump and signal combiner. The dispersion of both two DC-TDFs is dominated by the material dispersion of host material silica, generally exhibiting large negative values at the 2 μm regime, similar to the SMF-28e. A 20 cm long SMF-28e pigtail is finally spliced at the output not only

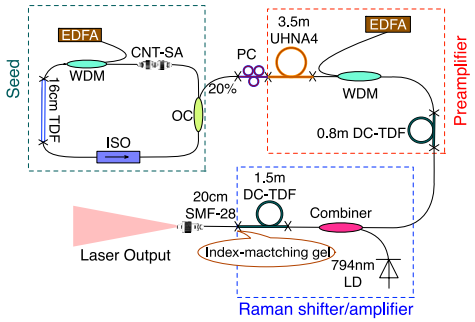

Fig. 1. Experimental setup. EDFA: erbium-doped fiber amplifier; WDM: wavelength division multiplexer; TDF: thulium-doped fiber; DC-TDF: double cladding TDF; ISO: isolator; OC: optical coupler; PC: polarization controller; CNT-SA: carbon nanotube based saturable absorber; LD: laser diode.

for a truly single mode operation, but also for stripping cladding pump power. To further deplete the residual pump light, near the splicing point of output pigtail, the bared fiber is coated with high index-matching gel (see Fig. 1), leading to >30 dB depletion of cladding pump light. The whole system is constructed by silica fibers and can be directly fuse-spliced.

Above a pump power of 213 mW of seed laser, self-start mode-locking operation with 55.42 MHz pulse repetition rate is achieved. The pump power can be increased to up to 245 mW without pulse breaking. Because of the large modulation depth of our CNT-SA, no PC is required to initialize and stabilize the mode-locking operation, confirming the reliability of our seed oscillator. Note that we do not notice any significant pulse performance improvement with an additional PC inside the seed laser. Therefore, in order to make the seed laser compact and stable, we don't put the PC into the cavity. We use the seed pulses at 215 mW pump as input signal for the following amplifier. The output power of the seed laser is measured as 9.3 mW. Figs. 2(a-b) shows the seed pulse features, which are measured with a FROG device (Mesa-photonics) and an optical spectrum analyzer (Yokogawa AQ6375). We observe good agreement between the retrieved and measured optical spectrum (see Fig. 2(a)), with the exception of a mismatch at sidebands. This is because the sidebands arising from dispersive waves typically have low intensity [28], leading to too weak second harmonic generation to be detected by the FROG device. The spectrum is centered at 1957 nm with a 6.8 nm FWHM. The retrieved pulse duration is 725 fs with a time-bandwidth product (TBP) of 0.39, close to the Fourier-transform limit of 590 fs, as shown in Fig. 2(b).

After propagating through the PC and DCF, the pulses have an average power of 4.6 mW, and are stretched to ~1.88 ps with a virtually unchanged spectrum (See Figs. 2(c-d)). The parabolic-like shape of temporal phase $\phi(t)$ (Fig. 2(d)) indicates that the stretched pulse has a positively linear chirp, as the instantaneous angular frequency of a pulse is determined by the phase, $\omega(t)=\omega_0-d\phi(t)/dt$, where ω_0 is the central angular frequency of light pulse. Pulse compression and amplification can therefore be simultaneously realized in the following DC-TDF with negative dispersion. With a 1.7 W pump power, the preamplifier can generate pulses with an average power of 46.1 mW. The spectral bandwidth is broadened to 18.5 nm, and the pulse width is compressed to 345 fs, see Figs. 2(e-f). The temporal phase in Fig. 2(f) implies that the pulse wing has uncompensated chirp, which could be further compressed in

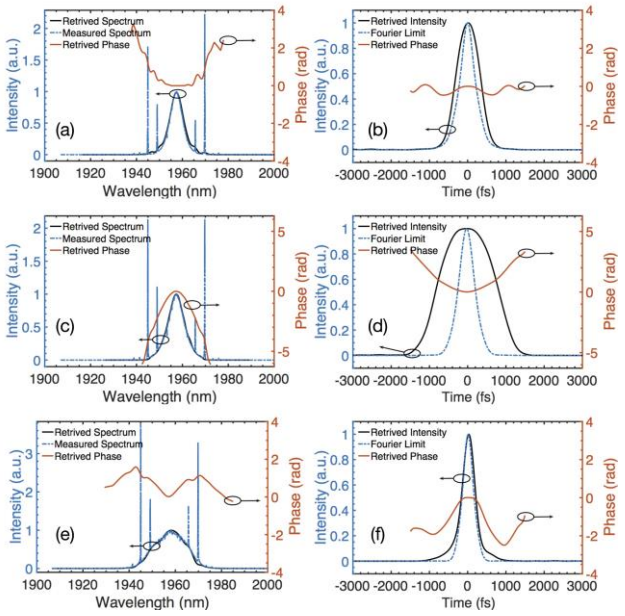

Fig. 2. Pulse characteristics of seed pulse (a), (b); stretched pulse (c), (d); pre-amplified pulse (e), (f). The blue dotted line indicates the measured spectrum in frequency domain or calculated Fourier-limit pulse in time domain; The black and orange solid lines indicate the retrieved spectra (or pulses) and their corresponding spectral phases (or temporal phases) from FROG device, respectively.

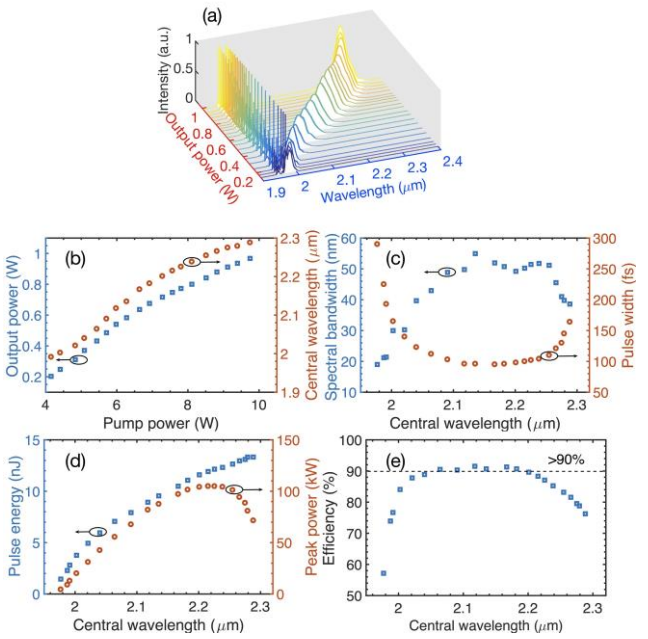

Fig. 3. (a) Wavelength evolution of Raman solitons. (b) The total output power of the system and the central wavelength of the solitons as a function of the pump power at 794 nm. (c) The spectral bandwidth and pulse width, (d) peak power and pulse energy, and (e) conversion efficiency of the Raman solitons as a function of central wavelength.

the passive fiber of combiner. By sending these compressed pulses into the Raman shifter, we could efficiently shift the frequency to long wavelength beyond 2.2 μm by neglecting the increasing absorption of host silica since the amount of SSFS is proportional to $1/\tau^4$[12], where τ is the pulse width.

Continuously wavelength-tunable Raman solitons are obtained as soon as the pump power of the second-stage amplifier is higher than 3.66 W, see Fig. 3(a). To clearly observe the Raman solitons, we normalize the spectral intensity to the strongest soliton peak at 2.29 μm, without displaying the full y-axis range for the sidebands associated with the seed spectrum. As the pump power is increased from 3.66 to 9.75 W, the central wavelength of Raman soliton gradually shifts from 1.98 to 2.29 μm, with the total output power increasing from 140.8 to 968 mW; Fig. 3(b). We note that Raman shifts to longer wavelength is possible if a higher pump power LD is used. However, this expected to be accompanied with the birth of distinguishable second tunable soliton and a spectral narrowing of the first soliton. Wavelength tunability of up to ~2.29 μm is contributed to the flat dispersion design in the pre-amplifier with dispersion compensation. We also note that the PC is only pre-adjusted to stabilize the Raman soliton and is not changed as the wavelength shifts. Long-term stability of wavelength shift and reproducibility of the results were observed during the 12-hour measurement period.

As the measurable wavelength of our FROG device is limited to up to 2188 nm, we use an autocorrelator (APE pulseCheck) to measure the soliton duration via slightly adjusting the crystal angle. The measured pulse duration and spectral width of the generated pulses vary between 95 and 290 fs, and, 19 and 54 nm, respectively, see Fig. 3(c). The majority of the Raman solitons have TBP < 0.36 over the whole tuning range. In the central wavelength range from 2.11-2.215 μm, the pulse durations are <100 fs. The energy of Raman solitons increases from 1.45 to 13.3 nJ with the increase in pump power; Fig. 3(d). In particular, solitons with >10 nJ could be achieved in the 2.16-2.29 μm tuning range. Assuming a sech² profile of the generated pulse, the peak power can be calculated from energy and duration according to $P_{peak} = 0.88 \cdot E_p / \tau_p$, where E_p is the pulse energy and τ_p is the pulse duration. More than 100 kW peak power (between 100 and 104 kW) is directly achieved across the 2.18-2.25 μm range (see Fig. 3(d)), due to the large core diameter (12 μm) of Raman amplifier together with decreasing nonlinearity (proportional to $(\lambda \cdot A_{eff})^{-1}$[12], where A_{eff} is the effective mode area) at the long wavelength regime.

We also calculate the conversion efficiency of Raman soliton, which varies between 57% and 91.5%, see Fig. 3(e). Relatively low efficiency <2 μm and >2.26 μm could be due to the incomplete shifting of Raman soliton and the increasing absorption of host silica, respectively. In the 2.06-2.18 μm tuning range, the conversion efficiency is >90%, exceeding the previous reported highest value of 62.5% [17] from a Raman-shifted Tm fiber laser. Both the Raman soliton energy and conversion efficiency are calculated by integrating the area under the spectral curve, as reported in Refs. [16, 17, 20]. We attribute this large efficiency to the use of large core DC-TDF, which has relatively large negative dispersion together with low nonlinearity. Thus, energy conversion to most red-shifted soliton is maximized by decreasing the number of excited fundamental solitons [29].

To further understand the properties of the generated pulses, we record the results presented in Fig. 4 at 5.7 W pump power using the FROG device. The calculated FROG error is 0.6% between the measured (Fig. 4(a)) and retrieved (Fig. 4(b)) FROG traces. Fig. 4(c) gives the corresponding optical spectra, exhibiting

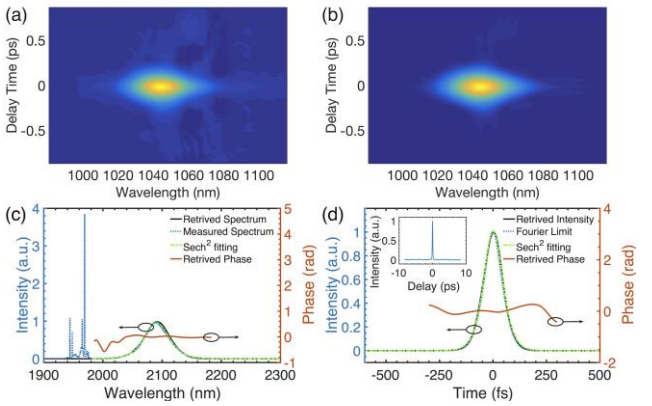

Fig. 4. (a) Measured and (b) retrieved FROG trace from the Raman soliton. (c) Retrieved spectral intensity (black solid) and corresponding phase (orange solid), and the independently measured spectrum (blue dotted), fitting with sech² profile (green dashed). (d) Retrieved temporal pulse (black solid) fitting with sech² profile (green dashed) and corresponding phase (orange solid), and calculated Fourier-limit pulse (blue dotted). Inset: autocorrelation trace.

good agreement between them. The spectrum is centered at 2.09 μm with a bandwidth of ~50 nm. The retrieved pulse has ~103 fs duration, with a TBP of 0.35, close to the calculated Fourier-limit pulse (Fig. 4(d)). Both the spectrum and pulse fit well with the sech² profile, typical of soliton characteristics. Wide span autocorrelation trace in the inset of Fig. 4(d) shows neglected seed pulses, indicating that most energy is shifted to the Raman soliton, confirming high conversion efficiency. We note that during the reviewing process of our manuscript, we came across two recent publications with similar results [30, 31].

In conclusion, Raman solitons with wavelength tunability of 310 nm from 1.98 to 2.29 μm, a minimum pulse duration of 95 fs, and a maximum pulse energy of 13.3 nJ are directly generated from an all-silica-fiber Tm laser system. By employing a CPA structure with dispersion compensation in the preamplifier, the SSFS is effectively extended to up to ~2.29 μm by overcoming the host silica material absorption. Both Raman amplifier and shifter are realized by a DC-TDF with 12 μm core diameter, leading to generation of high energy and high Raman conversion efficiency. With energy conversion to most red-shifted soliton as high as 91.5%, Raman solitons with > 10 nJ energy beyond 2.22 μm from an all-silica-fiber tunable single-soliton-pulse source are reported for the first time. Our all-fiber based, broadly tunable femtosecond source in 2 μm region could facilitate various mid-IR applications, including gas sensing and high resolution ultrafast spectroscopy.

Funding. National Natural Science Foundation of China (NSFC) (61605122); Natural Science Foundation of Guangdong Province (2016A030310049); Shenzhen Science and Technology Program (KQJSCX20160226194031, JCYJ20150324140036862); EPSRC (EP/L016087/1); European Union's 7th Framework Programme (631610); Royal Academy of Engineering (Graphlex); Academy of Finland (276376, 284548, 295777, 304666); TEKES (OPEC).

References

1. A. Schliesser, N. Picque, and T. W. Hansch, Nat. Photon. **6**, 440 (2012).
2. J. E. Bertie and Z. Lan, Appl. Spectroscopy **50**, 1047 (1996).
3. C. W. Rudy, M. J. F. Digonnet, and R. L. Byer, Opt. Fiber Technol. **20**, 642 (2014).
4. L. E. Nelson, E. P. Ippen, and H. A. Haus, Appl. Phys. Lett. **67**, 19 (1995).
5. S. D. Jackson, Nat. Photon. **6**, 423 (2012).
6. F. Haxsen, A. Wienke, D. Wandt, J. Neumann, and D. Kracht, Opt. Fiber Technol. **20**, 650 (2014).
7. B. Sun, J. Luo, Z. Yan, K. Liu, J. Ji, Y. Zhang, Q. J. Wang, and X. Yu, Opt. Express **25**, 8997 (2017).
8. G. Imeshev and M. Fermann, Opt. Express **13**, 7424 (2005).
9. Y. Meng, Y. Li, Y. Xu, and F. Wang, Sci Rep-Uk **7**, 45109 (2017).
10. A. E. Bednyakova, S. A. Babin, D. S. Kharenko, E. V. Podivilov, M. P. Fedoruk, V. L. Kalashnikov, and A. Apolonski, Opt. Express **21**, 20556 (2013).
11. S. A. Babin, E. V. Podivilov, D. S. Kharenko, A. E. Bednyakova, M. P. Fedoruk, V. L. Kalashnikov, and A. Apolonski, Nat. Commun. **5**, 4653 (2014).
12. G. Agrawal, *Nonlinear Fiber Optics,* 5th ed. (Academic Press, 2012).
13. M. Zhang, E. J. R. Kelleher, T. H. Runcorn, V. M. Mashinsky, O. I. Medvedkov, E. M. Dianov, D. Popa, S. Milana, T. Hasan, Z. Sun, F. Bonaccorso, Z. Jiang, E. Flahaut, B. H. Chapman, A. C. Ferrari, S. V. Popov, and J. R. Taylor, Opt. Express **21**, 23261 (2013).
14. M. Y. Koptev, E. A. Anashkina, A. V. Andrianov, V. V. Dorofeev, A. F. Kosolapov, S. V. Muravyev, and A. V. Kim, Opt. Lett. **40**, 4094 (2015).
15. Y. Tang, L. G. Wright, K. Charan, T. Wang, C. Xu, and F. W. Wise, Optica **3**, 948 (2016).
16. D. Klimentov, N. Tolstik, V. V. Dvoyrin, R. Richter, and I. T. Sorokina, J. Lightwave Technol. **34**, 4847 (2016).
17. Kivisto, x, S., T. Hakulinen, M. Guina, and O. G. Okhotnikov, IEEE Photon. Technol. Lett. **19**, 934 (2007).
18. R. Sims, P. Kadwani, L. Shah, and M. Richardson, in *Advances in Optical Materials*, OSA Technical Digest (CD) (Optical Society of America, 2011), ATuD4.
19. J. Jiang, A. Ruehl, I. Hartl, and M. E. Fermann, in *CLEO:2011 - Laser Applications to Photonic Applications*, OSA Technical Digest (CD) (Optical Society of America, 2011), CThBB5.
20. V. V. Dvoyrin, D. Klimentov, I. T. E. D. E.-Z. M. Sorokina, and I. Sorokina, in *Advanced Solid-State Lasers Congress*, OSA Technical Digest (online) (Optical Society of America, 2013), MTh1C.2.
21. D. Klimentov, V. Dvoyrin, N. Tolstik, and I. T. Sorokina, in *High-Brightness Sources and Light-Driven Interactions*, OSA technical Digest (online) (Optical Society of America, 2016), MM6C.2.
22. H. Hoogland, S. Wittek, W. Hänsel, S. Stark, and R. Holzwarth, Opt. Lett. **39**, 6735 (2014).
23. J. Wang, X. Liang, G. Hu, Z. Zheng, S. Lin, D. Ouyang, X. Wu, P. Yan, S. Ruan, Z. Sun, and T. Hasan, Sci. Rep. **6**, 28885 (2016).
24. T. Hasan, Z. Sun, F. Wang, F. Bonaccorso, P. H. Tan, A. G. Rozhin, and A. C. Ferrari, Adv. Mater. **21**, 3874 (2009).
25. M. Chernysheva, A. Bednyakova, M. Al Araimi, R. C. T. Howe, G. Hu, T. Hasan, A. Gambetta, G. Galzerano, M. Rümmeli, and A. Rozhin, Sci. Rep. **7**, 44314 (2017).
26. Y. Tang, A. Chong, and F. W. Wise, Opt. Lett. **40**, 2361 (2015).
27. Q. Wang, T. Chen, M. Li, B. Zhang, Y. Lu, and K. P. Chen, Appl. Phys. Lett. **103**, 011103 (2013).
28. M. L. Dennis and I. N. Duling, III, IEEE J. Quantum Electron. **30**, 1469 (1994).
29. J. M. Dudley, G. Genty, and S. Coen, Rev. Mod. Phys. **78**, 1135 (2006).
30. J. Luo, B. Sun, J. Ji, E. L. Tan, Y. Zhang, and X. Yu, Opt. Lett. **42**, 1568 (2017).
31. P. Wang, H. Shi, F. Tan, and P. Wang, Opt. Express **25**, 16643 (2017).

References with titles

1. A. Schliesser, N. Picque, and T. W. Hansch, "Mid-infrared frequency combs," Nat. Photon. **6**, 440-449 (2012).
2. J. E. Bertie and Z. Lan, "Infrared Intensities of Liquids XX: The Intensity of the OH Stretching Band of Liquid Water Revisited, and the Best Current Values of the Optical Constants of H2O(l) at 25°C between 15,000 and 1 cm−1," Appl. Spectroscopy **50**, 1047-1057 (1996).
3. C. W. Rudy, M. J. F. Digonnet, and R. L. Byer, "Advances in 2-μm Tm-doped mode-locked fiber lasers," Opt. Fiber Technol. **20**, 642-649 (2014).
4. L. E. Nelson, E. P. Ippen, and H. A. Haus, "Broadly tunable sub-500 fs pulses from an additive-pulse mode-locked thulium-doped fiber ring laser," Appl. Phys. Lett. **67**, 19-21 (1995).
5. S. D. Jackson, "Towards high-power mid-infrared emission from a fibre laser," Nat. Photon. **6**, 423-431 (2012).
6. F. Haxsen, A. Wienke, D. Wandt, J. Neumann, and D. Kracht, "Tm-doped mode-locked fiber lasers," Opt. Fiber Technol. **20**, 650-656 (2014).
7. B. Sun, J. Luo, Z. Yan, K. Liu, J. Ji, Y. Zhang, Q. J. Wang, and X. Yu, "1867-2010 nm tunable femtosecond thulium-doped all-fiber laser," Opt. Express **25**, 8997-9002 (2017).
8. G. Imeshev and M. Fermann, "230-kW peak power femtosecond pulses from a high power tunable source based on amplification in Tm-doped fiber," Opt. Express **13**, 7424-7431 (2005).
9. Y. Meng, Y. Li, Y. Xu, and F. Wang, "Carbon Nanotube Mode-Locked Thulium Fiber Laser With 200 nm Tuning Range," Sci Rep-Uk **7**, 45109 (2017).
10. A. E. Bednyakova, S. A. Babin, D. S. Kharenko, E. V. Podivilov, M. P. Fedoruk, V. L. Kalashnikov, and A. Apolonski, "Evolution of dissipative solitons in a fiber laser oscillator in the presence of strong Raman scattering," Opt. Express **21**, 20556-20564 (2013).
11. S. A. Babin, E. V. Podivilov, D. S. Kharenko, A. E. Bednyakova, M. P. Fedoruk, V. L. Kalashnikov, and A. Apolonski, "Multicolour nonlinearly bound chirped dissipative solitons," Nat. Commun. **5**, 4653 (2014).
12. G. Agrawal, *Nonlinear Fiber Optics,* 5th ed. (Academic Press, 2012).
13. M. Zhang, E. J. R. Kelleher, T. H. Runcorn, V. M. Mashinsky, O. I. Medvedkov, E. M. Dianov, D. Popa, S. Milana, T. Hasan, Z. Sun, F. Bonaccorso, Z. Jiang, E. Flahaut, B. H. Chapman, A. C. Ferrari, S. V. Popov, and J. R. Taylor, "Mid-infrared Raman-soliton continuum pumped by a nanotube-mode-locked sub-picosecond Tm-doped MOPFA," Opt. Express **21**, 23261-23271 (2013).
14. M. Y. Koptev, E. A. Anashkina, A. V. Andrianov, V. V. Dorofeev, A. F. Kosolapov, S. V. Muravyev, and A. V. Kim, "Widely tunable mid-infrared fiber laser source based on soliton self-frequency shift in microstructured tellurite fiber," Opt. Lett. **40**, 4094-4097 (2015).
15. Y. Tang, L. G. Wright, K. Charan, T. Wang, C. Xu, and F. W. Wise, "Generation of intense 100 fs solitons tunable from 2 to 4.3 μm in fluoride fiber," Optica **3**, 948-951 (2016).
16. D. Klimentov, N. Tolstik, V. V. Dvoyrin, R. Richter, and I. T. Sorokina, "Flat-Top Supercontinuum and Tunable Femtosecond Fiber Laser Sources at 1.9-2.5 μm," J. Lightwave Technol. **34**, 4847-4855 (2016).
17. Kivisto, x, S., T. Hakulinen, M. Guina, and O. G. Okhotnikov, "Tunable Raman Soliton Source Using Mode-Locked Tm-Ho Fiber Laser," IEEE Photon. Technol. Lett. **19**, 934-936 (2007).
18. R. Sims, P. Kadwani, L. Shah, and M. Richardson, "All Thulium Fiber CPA System with 107 fs Pulse Duration and 42 nm Bandwidth," in *Advances in Optical Materials*, OSA Technical Digest (CD) (Optical Society of America, 2011), ATuD4.
19. J. Jiang, A. Ruehl, I. Hartl, and M. E. Fermann, "Tunable Coherent Raman Soliton Generation with a Tm-Fiber System," in *CLEO:2011 - Laser Applications to Photonic Applications*, OSA Technical Digest (CD) (Optical Society of America, 2011), CThBB5.
20. V. V. Dvoyrin, D. Klimentov, I. T. E. D. E.-Z. M. Sorokina, and I. Sorokina, "3W Raman Soliton Tunable between 2-2.2 μm in Tm-Doped Fiber MOPA," in *Advanced Solid-State Lasers Congress*, OSA Technical Digest (online) (Optical Society of America, 2013), MTh1C.2.
21. D. Klimentov, V. Dvoyrin, N. Tolstik, and I. T. Sorokina, "Raman Soliton Fiber Lasers Tunable between 1.98 - 2.22 μm," in *High-Brightness Sources and Light-Driven Interactions*, OSA technical Digest (online) (Optical Society of America, 2016), MM6C.2.
22. H. Hoogland, S. Wittek, W. Hänsel, S. Stark, and R. Holzwarth, "Fiber chirped pulse amplifier at 2.08 μm emitting 383-fs pulses at 10 nJ and 7 MHz," Opt. Lett. **39**, 6735-6738 (2014).
23. J. Wang, X. Liang, G. Hu, Z. Zheng, S. Lin, D. Ouyang, X. Wu, P. Yan, S. Ruan, Z. Sun, and T. Hasan, "152 fs nanotube-mode-locked thulium-doped all-fiber laser," Sci. Rep. **6**, 28885 (2016).
24. T. Hasan, Z. Sun, F. Wang, F. Bonaccorso, P. H. Tan, A. G. Rozhin, and A. C. Ferrari, "Nanotube–polymer composites for ultrafast photonics," Adv Mater **21**, 3874-3899 (2009).
25. M. Chernysheva, A. Bednyakova, M. Al Araimi, R. C. T. Howe, G. Hu, T. Hasan, A. Gambetta, G. Galzerano, M. Rümmeli, and A. Rozhin, "Double-Wall Carbon Nanotube Hybrid Mode-Locker in Tm-doped Fibre Laser: A Novel Mechanism for Robust Bound-State Solitons Generation," Sci. Rep. **7**, 44314 (2017).
26. Y. Tang, A. Chong, and F. W. Wise, "Generation of 8 nJ pulses from a normal-dispersion thulium fiber laser," Opt. Lett. **40**, 2361-2364 (2015).
27. Q. Wang, T. Chen, M. Li, B. Zhang, Y. Lu, and K. P. Chen, "All-fiber ultrafast thulium-doped fiber ring laser with dissipative soliton and noise-like output in normal dispersion by single-wall carbon nanotubes," Appl. Phys. Lett. **103**, 011103 (2013).
28. M. L. Dennis and I. N. Duling, III, "Experimental study of sideband generation in femtosecond fiber lasers," IEEE J. Quantum Electron. **30**, 1469-1477 (1994).
29. J. M. Dudley, G. Genty, and S. Coen, "Supercontinuum generation in photonic crystal fiber," Rev. Mod. Phys. **78**, 1135-1184 (2006).
30. J. Luo, B. Sun, J. Ji, E. L. Tan, Y. Zhang, and X. Yu, "High-efficiency femtosecond Raman soliton generation with a tunable wavelength beyond 2 μm," Opt. Lett. **42**, 1568-1571 (2017).
31. P. Wang, H. Shi, F. Tan, and P. Wang, "Enhanced tunable Raman soliton source between 1.9 and 2.36 μm in a Tm-doped fiber amplifier," Opt. Express **25**, 16643-16651 (2017).